Theriogenology 205 (2023) 79–86

Contents lists available at ScienceDirect

Theriogenology

journal homepage: www.theriojournal.com

Characteristics of size-exclusion chromatography enriched porcine follicular fluid extracellular vesicles

Kinga Kamińska [a, b], Kasun Godakumara [c, d], Bianka Świderska [e], Agata Malinowska [e], Getnet Midekessa [c, d], Kamila Sofińska [f], Jakub Barbasz [g], Alireza Fazeli [c, d, h], Malgorzata Grzesiak [b, *]

[a] Doctoral School of Exact and Natural Sciences, Jagiellonian University, Krakow, Poland
[b] Department of Endocrinology, Institute of Zoology and Biomedical Research, Faculty of Biology, Jagiellonian University, Gronostajowa 9, 30-387, Krakow, Poland
[c] Institute of Veterinary Medicine and Animal Sciences, Estonian University of Life Sciences, Kreutzwaldi 62, 51006, Tartu, Estonia
[d] Department of Pathophysiology, Institute of Biomedicine and Translational Medicine, University of Tartu, Ravila St. 14b, 50411, Tartu, Estonia
[e] Mass Spectrometry Laboratory, Institute of Biochemistry and Biophysics, Polish Academy of Sciences, Warsaw, Pawinskiego 5a, 02-106, Warszawa, Poland
[f] M. Smoluchowski Institute of Physics, Faculty of Physics, Astronomy and Applied Computer Science, Jagiellonian University, Łojasiewicza 11, 30-348, Krakow, Poland
[g] Jerzy Haber Institute of Catalysis and Surface Chemistry, Polish Academy of Sciences, Niezapominajek 8, 30-239, Krakow, Poland
[h] Academic Unit of Reproductive and Developmental Medicine, Department of Oncology and Metabolism, Medical School, University of Sheffield, Sheffield, S10 2SF, UK

ARTICLE INFO

Article history:
Received 8 February 2023
Received in revised form
20 March 2023
Accepted 11 April 2023
Available online 14 April 2023

Keywords:
Extracellular vesicles
Size-exclusion chromatography
Nanoparticle Tracking Analysis
Atomic Force Microscopy
Ovary
Pig

ABSTRACT

Extracellular vesicles (EVs) are membrane-bound nanoparticles that are released by different cell types and play a crucial role in the intercellular communication. They carry various biomolecular compounds such as DNA, RNA, proteins, and lipids. Given that EVs are a new element of the communication within the ovarian follicle, extensive research is needed to optimize method of their isolation. The aim of the study was to assess size-exclusion chromatography (SEC) as a tool for effective EVs isolation from porcine ovarian follicular fluid. The characterization of EVs was performed by nanoparticle tracking analysis, transmission electron microscopy, atomic force microscopy, mass spectrometry and Western blot. We determined EVs concentration, size distribution, zeta potential, morphology, purity, and marker proteins. Our results show that SEC is an effective method for isolation of EVs from porcine follicular fluid. They displayed predominantly exosome properties with sufficient purity and possibility for further functional analyses, including proteomics.

1. Introduction

Extracellular vesicles (EVs) represent a heterogeneous population of membrane-bound nanoparticles that are released by different cell types and play a crucial role in the intercellular communication [1]. According to their biogenesis, biophysical and biochemical properties, they are usually categorized as small (exosomes) or large (microvesicles/ectosomes, migrasomes, apoptotic bodies) EVs [2]. Exosomes size range from 50 to 150 nm, originate in the endosomal pathway *via* the inward membrane budding of multivesicular bodies and possess molecular markers such as tetraspanins (CD63, CD9, CD81), Alix, TSG101, and flotillin-1 [3]. Microvesicles are formed by a direct budding from the plasma membrane; their size ranges from 100 to 1000 nm, and protein cargo includes annexin A1, integrins, selectins and CD40 [4]. Finally, migrasomes and apoptotic bodies (up to a few microns) are released from migrating and apoptotic cells, respectively [2]. Additionally, recent evidence suggests that cancer cells secrete a population of large oncosomes [5], whereas other cell types release arrestin domain-containing protein-mediated microvesicles [6].

It was established that EVs constitute a new mechanism of communication within the female reproductive system under physiological and pathological conditions [7,8]. They have been identified in different body fluids such as follicular, oviductal, uterine and amniotic fluid as well as the originating tissues [9]. EVs

* Corresponding author.
E-mail address: m.e.grzesiak@uj.edu.pl (M. Grzesiak).

https://doi.org/10.1016/j.theriogenology.2023.04.010

might influence target cells and regulate follicular growth and oocyte maturation [10], implantation, maternal-embryo interface [11], and fetal growth [12] *via* their RNA, DNA, miRNA, protein and lipid cargo. Therefore, there is still a growing interest in understanding the detailed role of EVs in the female reproduction.

The ovarian follicle is a functional unit supporting the growth and maturation of the oocyte that requires extensive cell-to-cell communication between follicular cells [13]. The signaling between somatic cells and the oocyte is coordinated through different hormones and molecules residing in the follicular fluid, including EVs [14]. Studies on EVs isolated from human [15], bovine [16,17] and equine [18,19] follicular fluid revealed their involvement in the follicle growth and oocyte developmental competence through the regulation of granulosa cell proliferation, tight junction communication between follicular cells and cumulus-oocyte complex maturation. However, still little is known about the role of EVs in the porcine ovarian follicle.

There is a lack of a standardized method of EVs enrichment from ovarian follicular fluid that can provide EV enriched samples with standardized purity and functionality. The most widely used methods are differential ultracentrifugation and commercial kits based on precipitation [15,16,18–20]. These methods, however, are limited by their inability to completely or partially restore EVs functionality after ultracentrifugation and low specificity of EVs enrichment after precipitation [2]. Recently it has been proposed that differential centrifugation method combined with size-exclusion chromatography (SEC) might be an appropriate isolation method allowing further reliable transcriptomic and proteomic analyses of their carriers [21]. Therefore, the aim of the present investigation was to assess the SEC as a tool for effective EVs isolation from porcine ovarian follicular fluid. The quantity, quality, and physical properties of isolated EVs were determined by nanoparticle tracking analysis (NTA), transmission electron microscopy (TEM) and atomic force microscopy (AFM). Finally, the proteomic characterization of EVs by mass spectrometry (LC-MS) and Western blot was performed.

2. Material and methods

2.1. Collection of follicular fluid from porcine ovarian follicles

Follicular fluid was collected from healthy medium (3–6.9 mm in diameter; average diameter 5 mm) antral follicles obtained from sexually mature cross-bred gilts (Large White × Polish Landrace) [20]. Ovaries were harvested at a local slaughterhouse under veterinarian control. Stage of the estrous cycle was verified by ovarian morphology and corpus luteum quality according to Akins and Morrisette [22]. The ovaries in follicular phase were then transported to the laboratory in ice-cold phosphate-buffered saline (137 mM NaCl; 2.7 mM KCl; 10 mM Na_2HPO_4; and 1.8 mM KH_2PO_4; pH 7.4) with antibiotic (AAS, Sigma-Aldrich, St. Louis, MO, USA) within ~1 h of collection. Follicular fluid was aspirated by a syringe (1.5 mL volume of each sample; n = 6) and then centrifuged at 300×*g* at 4 °C for 10 min to remove cells. Next, the supernatant was centrifuged at 2000×*g* at 4 °C for 10 min, and at 5000×*g* at 4 °C for 10 min to remove cell debris and apoptotic bodies, respectively. Finally, the samples were concentrated to 500 μL using Amicon® Ultra-2ml centrifugal filter (10 kDa cut-off) (Merck Millipore, Burlington, MA, USA).

The use of animals was in accordance with the Act of January 15, 2015 on the Protection of Animals Used for Scientific or Educational Purposes and Directive 2010/63/EU of the European Parliament and the Council of September 22, 2010 on the protection of animals used for scientific purposes.

2.2. Extracellular vesicles isolation

EVs were isolated from porcine follicular fluid using the SEC as previously described [23]. Briefly, the isolation was performed using 10 cm benchtop columns (Econo-pac® Disposable chromatography column; Bio-Rad Laboratories Inc., Berkeley, CA, USA) filled with cross-linked 4% agarose matrix of 90 μm beads (Sepharose 4 fast flow™, GE HealthCare Bio-Sciences AB, Uppsala, Sweden). Twenty fractions (each 500 μL) were collected, and then the protein concentration within each fraction was determined using Bradford Protein Assay (Bio-Rad Laboratories Inc.) according to the manufacturer's protocol. Nanoparticle concentration in the fractions was measured using NTA as described in the subchapter *2.3*. As a result of this analysis, fractions 5–9 (2.5 mL) were pooled together and concentrated to 0.5 mL with Amicon® Ultra-2ml centrifugal filter (10 kDa cut-off) by centrifuging at 3000×*g* for 2 h at 4 °C (Fig. 1).

2.3. Nanoparticle tracking analysis

To determine EVs size and concentration, NTA was performed applying the ZetaView PMX 110 NTA instrument (Particle Metrix GmbH, Inning am Ammersee, Germany) with the corresponding ZetaView NTA software (8.04.02 SP2) for data analysis following Dissanayake et al. [24]. Before the measurements, the instrument was calibrated using a 100 nm polystyrene nanoparticles standard (Applied Microspheres BV, Leusden, The Netherlands, cat. no. 10100). The Brownian motion of each particle was visualized by a laser light scattering method, recorded by a camera and converted into size and concentration parameters using the Stokes-Einstein equation. Each EV sample was diluted with 1 × PBS (1:1000; cat. no. D8537, Sigma-Aldrich) to ensure that the concentration of particles in each sample was optimal, and then counted in three cycles at 11 points in the NTA flow cell. Following settings were utilized: sensitivity 85, shutter speed 70, and frame rate at 30 frames per second.

2.4. Zeta potential measurements

The zeta potential of EVs was performed by ZetaView PMX 110 according to previous studies [24,25]. Before the measurement, EV samples were adjusted to pH 7. Zeta potential was assessed at 22 °C under the following settings: cycles 5, sensitivity 85, shutter speed 70, and frame rate at 30 frames per second.

2.5. Transmission electron microscopy

To visualize EVs obtained from porcine follicular fluid, negative stained TEM was used with formvar coated, 300 mesh copper grids prepared for each EVs preparation using 2% uranyl acetate (Chemapol, Prague, Czech Republic). The JEOL JEM2100 HT transmission electron microscope was then used to observe the samples (JEOL, Tokyo, Japan).

2.6. Atomic force microscopy analysis

For AFM imaging, EVs were deposited on a highly oriented pyrolytic graphite (HOPG). Specifically, a 5 μL droplet of EVs solution prepared as described above, was casted on a freshly cleaved HOPG surface right before EVs deposition. After 5 min of incubation at room temperature, the sample was rinsed with ultrapure water and left to dry. AFM images of EVs were acquired in a tapping mode with a scanning rate of 0.5 Hz and 512 × 512 pixels using SmartSPM™ 1000 Scanning Probe Microscope (AIST-NT, Horiba, France) and RTESPA-150 probes (Bruker). Collected AFM images were processed using Gwydion [26] software (Version 2.51) *via*

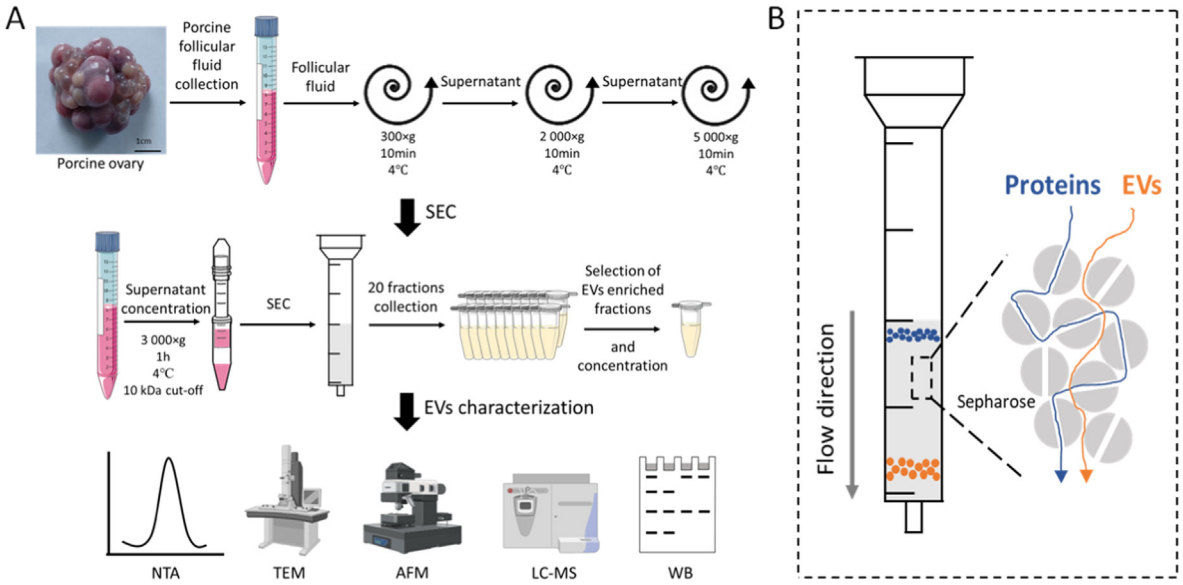

Fig. 1. Flow chart of the study design. (A) Extracellular vesicles (EVs) from porcine follicular fluid was isolated using size-exclusion chromatography (SEC). The collected porcine follicular fluid was loaded on a sepharose columns, 20 fractions were collected, selected for concentration and then analyzed by nanoparticle tracking analysis (NTA), transmission electron microscopy (TEM), atomic force microscopy (AFM), liquid chromatography mass spectrometry (LC-MS) and Western blot (WB). (B) Molecules are separated based on their size as they pass through the column and they are eluted in order of decreasing molecular weight.

flattening by a median of differences correction. To determine the diameter distribution of EVs, the dimensions were established from 1731 EVs present on AFM images.

2.7. Western blot analysis

Western blot was conducted on EV samples pooled from fractions 5–9. Proteins were precipitated by adding 900 μL of water, 1200 μL of methanol and 300 μL of chloroform. The solution was vortexed and centrifuged at 9000×*g* at 4 °C for 5 min. Then, the top layer was removed and precipitated proteins were washed with 900 μL of methanol and centrifuged again at 9000×*g* at 4 °C for 10 min. The pellets were air-dried, resuspended in PBS and protein concentration was measured by Bradford assay. Proteins (20 μg from each group) were suspended in reducing Laemmli buffer (Bio-Rad Laboratories Inc.) and incubated at 95 °C for 5 min. Protein samples were separated by 12% SDS-polyacrylamide gel and transferred to PVDF membranes (Sigma-Aldrich, St. Louis, MO, USA) using a semi-dry Trans-Blot Turbo Transfer System (Bio-Rad Laboratories Inc.). The membranes were washed and blocked in 5% non-fat dry milk containing 1% BSA and 0.1% Tween20. Then membranes were incubated with the primary anti-CD63 antibody (cat. no 10628D, 1:500, Invitrogen, Carlsbad, CA, USA), anti-Apo-A1 antibody (cat. no DF6264, 1:500, Affinity Biosciences Inc., Cincinnati, OH, USA) and anti-β-actin (cat. no A2228, 1:4000, Sigma-Aldrich) overnight at 4 °C followed by incubation with horseradish peroxidase-conjugated goat anti-rabbit secondary antibody (cat. no 31460, 1:3000, Invitrogen) or goat anti-mouse secondary antibody (cat. no 170-6516, 1:3000, Bio-Rad Laboratories Inc.) for 1.5 h at room temperature. Bands were detected by chemiluminescence using Western blotting Luminol Reagent (Bio-Rad Laboratories Inc.) and visualized using the ChemiDocTM XRS + System (Bio-Rad Laboratories Inc.).

2.8. Immunofluorescence

Immunofluorescence labeling was performed as previously described [27]. Sections were deparaffinized, rehydrated, antigen retrieval and blocked using 5% normal goat serum prior to overnight incubation with primary anti-CD63 antibody (1:50, Invitrogen). Secondary antibody, Alexa Fluor™ 488-conjugated goat anti-mouse (cat. no A11001, 1:100, Invitrogen) was applied and incubated for 1.5 h in the darkness at room temperature. Finally, sections were mounted in Vectashield Antifade Mounting Medium (Vector Lab., Burlingame, CA, USA) and visualized with an epifluorescence microscope Nikon Eclipse Ni–U (Nikon, Tokyo, Japan) with corresponding software.

2.9. Mass spectrometry and data analysis

EVs suspended in 50 μL of PBS were lysed by the addition of digestion buffer to the final concentrations of 50 mM triethylammonium bicarbonate (TEAB), 5% trifluoroethanol (TFE), 10 mM Tris(2-carboxyethyl)phosphine (TCEP) and 40 mM 2-chloroacetamide (CAA). Samples were incubated at 95 °C on vortex for 15 min and sonicated in ultrasound bath at 60 °C for another 15 min. Digestion was performed at 37 °C overnight with 1 μg of trypsin (Promega, Madison, USA). After digestion, peptides were diluted to 100 μl with 50 mM TEAB and acidified to a final concentration of 0.1% formic acid (FA).

Samples were analyzed using LC-MS system composed of Evosep One (Evosep Biosystems, Odense, Danemark) coupled to an Orbitrap Exploris 480 mass spectrometer (Thermo Fisher Scientific, Bremen, Germany) *via* Flex nanoESI ion source (Thermo Scientific). Samples were loaded onto disposable Evotips C18 trap columns (Evosep Biosystems) according to the manufacturer protocol with minor modifications. Briefly, Evotips were activated with 25 μL of solvent B (solvent B: 0.1% formic acid in acetonitrile) by 1 min centrifugation at 600*g* followed by 2 min incubation in 2-propanol. After equilibration with 25 μL of solvent A, 40 μL of each sample was loaded onto the solid phase. Bound peptides were washed twice with 100 μL and covered with 200 μL of solvent A. Chromatography was carried out at a flow rate 250 nL/min using the 88 min (15 samples per day) preformed gradient on EV1106 analytical column (Dr Maisch C18 AQ, 1.9 μm beads, 150 μm ID, 15 cm long, Evosep Biosystems). Data was acquired in positive mode with a data-

dependent method using the following parameters. MS1 resolution was set at 60 000 with a normalized AGC target 300%, Auto maximum inject time and a scan range of 300–1600 m/z. For MS2, resolution was set at 15 000 with a Standard normalized AGC target, Auto maximum inject time and top 40 precursors within an isolation window of 1.6 m/z considered for MS/MS analysis. Dynamic exclusion was set at 20 s with allowed mass tolerance of ±10 ppm and the precursor intensity threshold at 5e3. Precursor were fragmented in HCD mode with normalized collision energy of 30%. Spray voltage was set to 2.1 kV, funnel RF level at 40, and heated capillary temperature at 275 °C.

Raw data files were analyzed in Proteome Discoverer 2.4.0.305 software (Thermo Scientific) using Sequest search engine. The data were searched against the *Sus scrofa* full UniProt database (taxonomy ID = 9823, version 2021_04) and common contaminants PD database (version 2015_05). Precursor and fragment mass tolerances were set to 10 ppm and 0.02 Da, respectively. Enzyme specificity was set to trypsin with a maximum of two missed cleavages. Carbamidomethylation (C) was defined as fixed modification, oxidation (M), N-terminal protein acetylation and Methionine loss as variable modifications. Peptide false discovery rate (FDR) was set to 1% using Percolator.

3. Results and discussion

The proper ovarian follicle development leading to successful ovulation is coordinated by a set of complex interactions between follicular somatic cells and the oocyte; and requires the exchange of various molecules. Besides well-known hormonal signals, EVs are considered as a crucial element of this intrafollicular communication [13]. Despite the growing importance, still little is known about EVs mode of action within the mammalian ovarian follicle that is warranted mainly by their molecular cargo. Therefore, the ability to isolate EVs from follicular fluid and maintain their biological functionality appears to be of paramount importance. The present study aimed to assess the efficiency of SEC as a useful method for EVs isolation from ovarian follicles of the pig that represents the farm animal species with small volume of follicular fluid per follicle.

To determine whether porcine ovarian follicle could be a source of EVs in follicular fluid, we performed immunofluorescent localization of tetraspanin CD63, which is a reliable marker of exosomes [28]. The positive immunofluorescent signal was observed in the cytoplasm of the granulosa cells (Fig. 3E), confirming that they could secrete EVs into follicular fluid.

In the present study, EVs from porcine follicular fluid were isolated using SEC and analyzed by NTA to determine which SEC fractions contain the highest concentration of particles. Twenty fractions of 500 μL were collected from the SEC column in three biological replicates. Fractions 5–9 contained the highest number of EVs ranging from 1.4×10^{10}/mL to 5.2×10^{10}/mL, peaking in the fraction 6. Further fractions (10–20) contained relatively low EVs amount. To assess whether the SEC fractions are contaminated by proteins, the protein concentration in each fraction was measured using Bradford Protein Assay. We found that the protein concentration began to increase significantly after 9th fraction, whereas earlier ones (1–8) had none or minimal protein contamination (Fig. 2). Therefore, only fractions 5–9 were concentrated into one EV sample and used for further analyses.

To characterize porcine follicular fluid-derived EVs population, we performed NTA analysis of the concentration and size range of particles. The mean particle concentration in the EVs sample was $1.1 \times 10^{11} \pm 4.3 \times 10^{10}$/mL (Fig. 3B). As shown in Fig. 3A, the size distribution of isolated vesicles ranged between approximately 30 and 480 nm, indicating the presence of heterogeneous EVs population in the porcine follicular fluid. The vast majority of these particles were under 300 nm in diameter and a mean size was 148.35 nm, which corresponded to the exosome subpopulation [29]. Concordantly, similar results were obtained recently on EVs isolated from porcine ovarian follicular fluid by commercial Total Exosome Isolation Reagent [20] and differential centrifugation [30]. In addition, Western blot analysis revealed that follicular fluid-derived EVs were positive for common EVs markers CD63 and β-actin (Fig. 3D). To further ascertain the morphology of particles, TEM analysis was performed (Fig. 4). We observed heterogeneous population of double layered membrane vesicles, displaying typical "cup-shaped" morphology [31]. TEM analysis showed that the isolated particles were EVs (around 30–200 nm), which confirmed the NTA findings on the heterogeneity of porcine follicular fluid-derived particles. We continued by determining the dimensional diversity of EVs using AFM. The AFM images of EVs deposited onto a highly oriented pyrolytic graphite (HOPG) surface are presented in Fig. 5A and B. Furthermore, based on collected AFM images, the diameter distribution of deposited particles was determined (Fig. 5C). Apart from those corresponded to the EVs size, we found

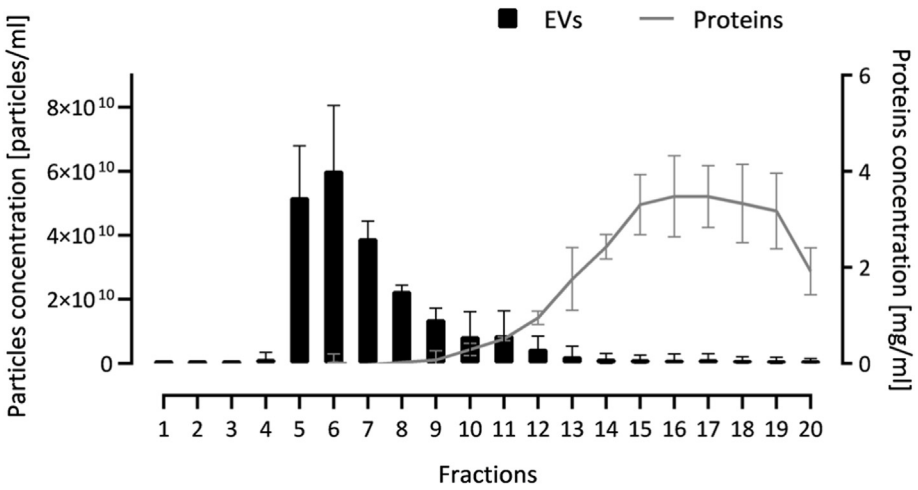

Fig. 2. Extracellular vesicles (EVs) and protein concentration in 20 fractions isolated by size-exclusion chromatography from porcine follicular fluid. In each fraction, EVs concentration was assessed using nanoparticle tracking analysis and the protein concentration was measured using Bradford Protein Assay. Data is shown as the mean ± standard deviation (SD) (n = 3).

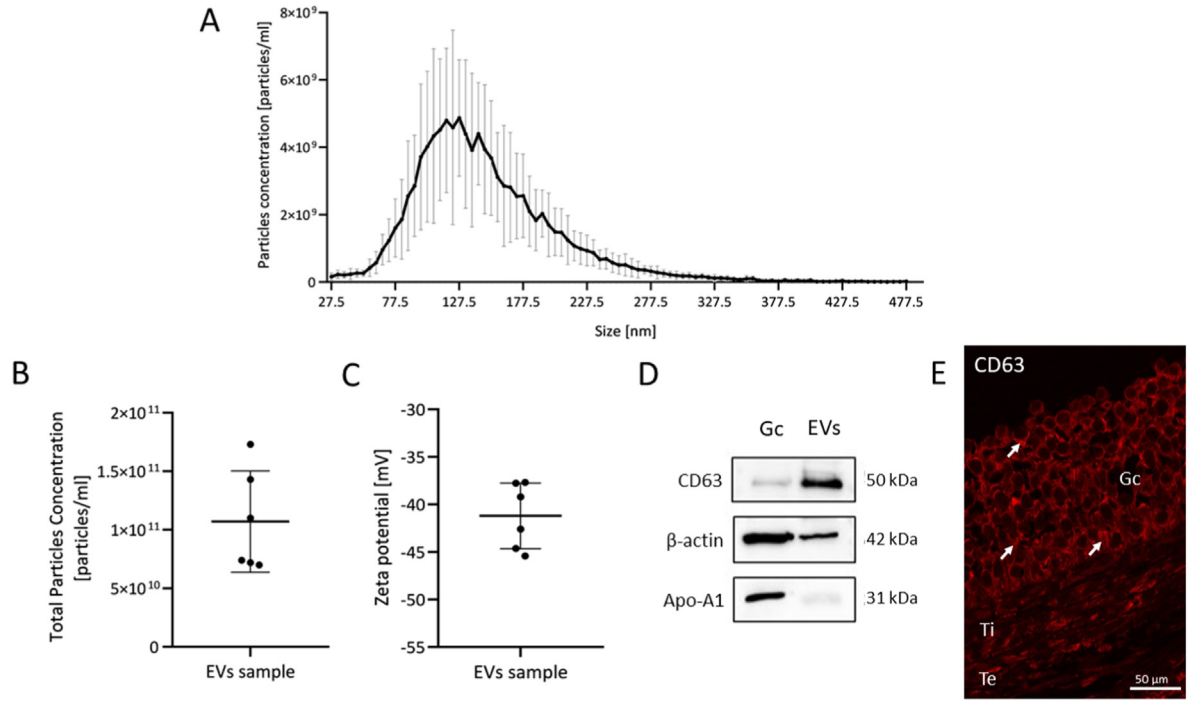

Fig. 3. Characterization of the extracellular vesicles (EVs) isolated from porcine follicular fluid. EVs size distribution (A), concentration (B) and zeta potential (C) were assessed by nanoparticle tracking analysis. Data is shown as the mean ± standard deviation (SD) (n = 6). Expression of CD63, β-actin and apolipoprotein A1 (Apo-A1) proteins in EVs samples and granulosa cell lysates (Gc) was demonstrated by Western blot (D). Immunofluorescence was used to confirm CD63 localization in porcine ovarian follicle (E). Positive signal (red) is marked by white arrows. Gc - granulosa cells; Ti - theca interna cells; Te -theca externa cells. (For interpretation of the references to colour in this figure legend, the reader is referred to the Web version of this article.)

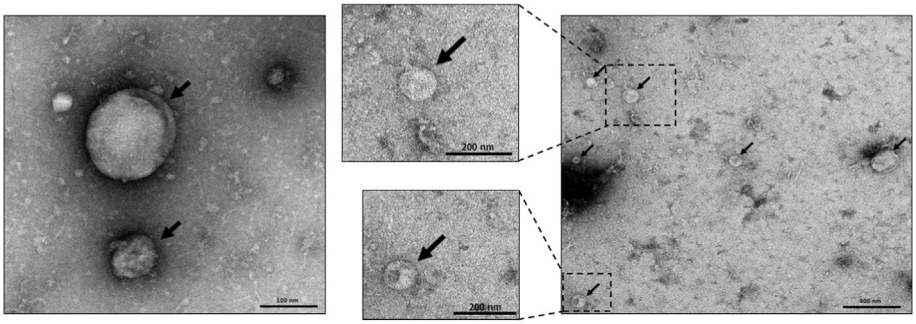

Fig. 4. Representative transmission electron microscopy images demonstrating extracellular vesicles (EVs) isolated from porcine follicular fluid and their morphology. Black arrows indicate "cup-shaped" EVs. Dotted inserts and the photo on the left represent the EVs at a higher magnification.

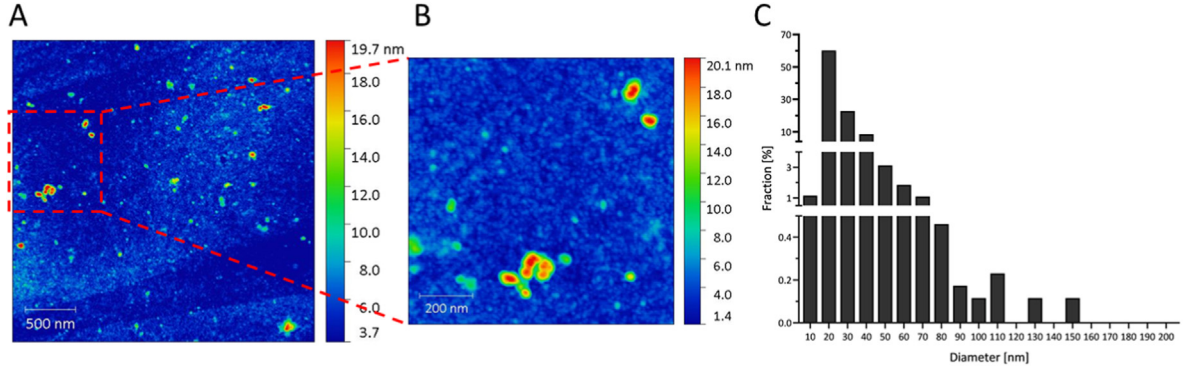

Fig. 5. Representative atomic force microscopy (AFM) images of extracellular vesicles (EVs) isolated from porcine follicular fluid deposited on a highly oriented pyrolytic graphite surface. (A) 3 × 3 μm^2 and (B) 1 × 1 μm^2 AFM image. (C) The distribution of EVs diameter determined from AFM images.

Table 1
List of marker proteins for extracellular vesicles (EVs) according to Menezes-Neto et al. [37] and their presence (yes)/absence (no) in EVs isolated form porcine follicular fluid using size-exclusion chromatography. The number of peptide spectral matches (#PSM) gives an estimation of the relative protein abundance.

EV marker proteins	Gene symbol	Identified	#PSM
Actin, cytoplasmic 1	ACTB	yes	104
Fructose-bisphosphate aldolase A	ALDOA	yes	19
Annexin A2	ANXA2	yes	52
Annexin A5	ANXA5	yes	63
Annexin A6	ANXA6	yes	88
CD63 antigen	CD63	yes	2
CD81 antigen	CD81	no	0
CD82 antigen	CD82	no	0
CD9 antigen	CD9	yes	1
Cofilin-1	CFL1	yes	27
Clathrin heavy chain 1	CLTC	yes	160
Elongation factor 1-alpha 1	EEF1A1	yes	39
Ezrin	EZR	yes	32
Fatty acid synthase	FASN	yes	15
Glyceraldehyde-3-phosphate dehydrogenase	GAPDH	yes	46
Rab GDP dissociation inhibitor beta	GDI2	yes	11
Heat shock cognate 71 kDa *protein*	HSPA8	yes	88
Lactadherin	MFGE8	yes	19
Moesin	MSN	yes	19
Programmed cell death 6-interacting protein	PDCD6IP	no	0
Phosphoglycerate kinase 1	PGK1	yes	35
Pyruvate kinase	PKM2	no	0
Peroxiredoxin-1	PRDX1	no	0
Ras-related protein Rap-1b	RAP1B	yes	8
Radixin	RDX	yes	10
Transforming protein RhoA	RHOA	yes	11
Rho-related GTP-binding protein RhoC	RHOC	yes	9
Syntenin-1	SDCBP	yes	7
Tumour susceptibility gene 101 protein	TSG101	no	0
14-3-3 protein beta/alpha	YWHAB	no	0
14-3-3 protein epsilon	YWHAE	no	0
14-3-3 protein gamma	YWHAG	yes	9
14-3-3 protein theta	YWHAQ	yes	9
14-3-3 protein zeta/delta	YWHAZ	yes	13

the abundant population of particles under 30 nm in diameter that was rarely observed in the NTA analysis. Follicular fluid is composed partly of secretions from the follicular cells, and partly of exudates from plasma [32]. Therefore, it also contains typical plasma proteins, including lipoproteins. AFM analysis conducted on plasma EVs isolated by ultracentrifugation revealed the presence of particles ~20–30 nm in diameter, which were discussed as lipoproteins [33]. EVs isolated from plasma can be covered with low-density lipoproteins (LDL) that easily stick to their hydrophobic surfaces and co-isolate with EVs [34]. On the other hand, high-density lipoproteins (HDL) have a density similar to EVs and could also be co-isolated [35]. Gan et al. [36] showed using AFM that the average diameter of LDL and HDL is less than 30 nm, that could explain results obtained in the present study. To confirm that, we used mass spectrometry (Supplementary Table 1) and detected apolipoprotein A1 (Apo-A1), a marker for HDL and chylomicrons. That was confirmed by Western blot (Fig. 3D), however very week expression of Apo-A1 protein was found in EV samples. Regarding another common lipoprotein markers, such as Apo-B and Apo-E, there were not detected by mass spectrometry (Supplementary Table 1).

To our knowledge, the physical properties of EVs isolated from porcine follicular fluid such as surface charge, have not so far been reported. Herein for the first time we assessed zeta potential, a useful indicator of colloidal stability of EVs in solution, determining their interaction with target cells and surrounding environment [25]. The measurement was conducted at pH = 7.0 using NTA equipment and the mean zeta potential of EVs was −41.2 ± 3.45 mV (Fig. 3C). Nanoparticles with low zeta potential between −20 and + 20 mV have a tendency to aggregate, whereas greater zeta potential indicates better stability in solution that is important for EVs uptake by target cells and their impact on various biological processes [37]. Thus, our zeta potential results indicate stability of isolated EVs in solution and with characteristics to avoid aggregation.

The next aim of this research was to provide proteomic characterization of EVs using mass spectrometry (Supplementary Table 1). According to proteomic data set, Table 1 shows 34 marker proteins for EVs followed by de Menezes-Neto et al. [38] and their presence in EVs isolated from porcine follicular fluid using SEC. These particles expressed several exosomal markers, such as tetraspanins CD63 and CD9, lactadherin (MFGE8) and Rab GTD dissociation inhibitor beta (GDI2), suggesting endosomal origin of examined EVs [39]. That is in agreement with NTA and TEM analyses, indicating the great proportion of exosomes among isolated EVs. Notably, β-actin (ACTB), annexins 2 (ANXA2), 5 (ANX5) and 6 (ANX6), clathrin heavy chain 1 (CLTC), glyceraldehyde-3-phosphate dehydrogenase (GAPDH) and heat shock cognate 71 kDa protein (HSPA8) were identified with a great number of peptide spectral matches (#PSM) between 46 and 160 (Table 1). Most contamination marker proteins originating from Golgi apparatus (130 kDa cis-Golgi matrix protein, GM130) or mitochondria (cytochrome *c*1, CYC1) were absent in follicular fluid-derived EVs samples. On the other hand, endoplasmic reticulum proteins, such as endoplasmin/grp94 (HSP90B1), and nuclear histones (HIST) were identified (Supplementary Table 1). According to Vesiclepedia (access on January 12, 2023; microvesicles.org), endoplasmin/grp94 and several histones have 306 and above 200 entries, respectively. That is comparable with common exosome marker proteins such as CD63, CD9 or ACTB. Similar results were presented by Benedikter et al. [21], who suggested that endoplasmin/grp94 might be an EVs associated protein, while histones could be specifically sorted to EVs.

4. Conclusions

To summing up, the protocol of EVs isolation from the porcine follicular fluid using SEC described in this study yields EVs population displaying predominantly exosome properties and markers. We demonstrated that this approach of EVs isolation from follicular fluid could provide particles with some lipoprotein contamination. However more than 2000 proteins were identified herein with mass spectrometry, indicating that the achieved EVs sample purity is sufficient for proteomic analysis. Taking into account the prominent role of EVs in the female reproduction, including folliculogenesis, oocyte maturation, fertilization, and embryo quality [40], as well as changes in the composition of EVs cargo during reproductive aging [41], providing the protocol of effective follicular fluid-derived EVs isolation could be a starting point for further functional research on improving the pig fertility.

CRediT authorship contribution statement

Kinga Kamińska: Investigation, Methodology, Validation, Conceptualization, Formal analysis, Funding acquisition, Visualization, Writing - original draft. **Kasun Godakumara:** Methodology, Writing – review & editing. **Bianka Świderska:** Investigation. **Agata Malinowska:** Investigation. **Getnet Midekessa:** Methodology, Writing – review & editing. **Kamila Sofińska:** Investigation, Writing – review & editing. **Jakub Barbasz:** Investigation, Writing – review & editing. **Alireza Fazeli:** Resources, Writing - review & editing. **Malgorzata Grzesiak:** Conceptualization, Methodology, Supervision, Funding acquisition, Visualization, Writing - original draft.

Acknowledgments

This work was supported by grants from the National Science Centre (NCN, Poland, grant no. 2019/35/O/NZ9/02678 to MG), the European Union's Horizon 2020 Research and Innovation Programme under grant agreement No 857418 COMBIVET, and partly by the Programme "Excellence Initiative-Research University" at the Jagiellonian University in Krakow, Poland (no. U1U/W18/NO/28.19 to KK). This work is a result of doctoral internship within NAWA Preludium Bis 1 founded by The Polish National Agency For Academic Exchange (NAWA) to KK.

The authors would like to thank the Department of Cell Biology and Imaging of the Institute of Zoology and Biomedical Research, the Jagiellonian University for the access to the transmission electron microscope (JEOL JEM 2100HT).

Appendix A. Supplementary data

Supplementary data to this article can be found online at https://doi.org/10.1016/j.theriogenology.2023.04.010.

References

[1] van Niel G, Carter DRF, Clayton A, Lambert DW, Raposo G, Vader P. Challenges and directions in studying cell-cell communication by extracellular vesicles. Nat Rev Mol Cell Biol 2022;20:369–82. https://doi.org/10.1038/s41580-022-00460-3.

[2] Salomon C, Das S, Erdbrügger U, Kalluri R, Kiang Lim S, Olefsky JM, Rice GE, Sahoo S, Andy Tao W, Vader P, Wang Q, Weaver AM. Extracellular vesicles and their emerging roles as cellular messengers in endocrinology: an endocrine society scientific statement. Endocr Rev 2022;43:441–68. https://doi.org/10.1210/endrev/bnac009.

[3] Bebelman MP, Smit MJ, Pegtel DM, Baglio SR. Biogenesis and function of extracellular vesicles in cancer. Pharmacol Ther 2018;188:1–11. https://doi.org/10.1016/j.jprot.2010.06.006.

[4] Yáñez-Mó M, Siljander PRM, Andreu Z, et al. Biological properties of extracellular vesicles and their physiological functions. J Extracell Vesicles 2015;4:27066. https://doi.org/10.3402/jev.v4.27066.

[5] Di Vizio D, Morello M, Dudley AC, et al. Large oncosomes in human prostate cancer tissues and in the circulation of mice with metastatic disease. Am J Pathol 2012;181:1573–84. https://doi.org/10.1016/j.ajpath.2012.07.030.

[6] Nabhan JF, Hu R, Oh RS, Cohen SN, Lu Q. Formation and release of arrestin domain-containing protein 1-mediated microvesicles (ARMMs) at plasma membrane by recruitment of TSG101 protein. Proc Natl Acad Sci U S A 2012;109:4146–51. https://doi.org/10.1073/pnas.1200448109.

[7] Simon C, Greening DW, Bolumar D, Balaguer N, Salamonsen LA, Vilella F. Extracellular vesicles in human reproduction in health and disease. Endocr Rev 2018;39:292–332. https://doi.org/10.1210/er.2017-00229.

[8] Aleksejeva E, Zarovni N, Dissanayake K, Godakumara K, Vigano P, Fazeli A, Jaakma Ü, Salumets A. Extracellular vesicle research in reproductive science: paving the way for clinical achievements. Biol Reprod 2022;106:408–24. https://doi.org/10.1093/biolre/ioab24.

[9] Foster BP, Balassa T, Benen TD, et al. Extracellular vesicles in blood, milk and body fluids of the female and male urogenital tract and with special regard to reproduction. Crit Rev Clin Lab Sci 2016;53:379–95. https://doi.org/10.1080/10408363.2016.1190682.

[10] da Silveira JC, de Ávila A, Garrett HL, Bruemmer JE, Winger QA, Bouma GJ. Cell-secreted vesicles containing microRNAs as regulators of gamete maturation. J Endocrinol 2018;236:R15–27. https://doi.org/10.1530/JOE-17-0200.

[11] Szuszkiewicz J, Myszczynski K, Reliszko ZP, Heifetz Y, Kaczmarek MM. Early steps of embryo implantation are regulated by exchange of extracellular vesicles between the embryo and the endometrium. Faseb J 2022;36:e22450. https://doi.org/10.1096/fj.202200677R.

[12] Karlsson O, Rodosthenous RS, Jara C, Brennan KJ, Wright RO, Baccarelli AA, Wright RJ. Detection of long non-coding RNAs in human breastmilk extracellular vesicles: implications for early child development. Epigenetics 2016;11:721–9. https://doi.org/10.1080/15592294.2016.1216285.

[13] Clarke HJ. Regulation of germ cell development by intercellular signaling in the mammalian ovarian follicle, 7. Wiley Interdiscip Rev Dev Biol; 2018. https://doi.org/10.1002/wdev.294. 10.1002/wdev.294.

[14] Di Pietro C. Exosome-mediated communication in the ovarian follicle. J Assist Reprod Genet 2016;33:303–11. https://doi.org/10.1007/s10815-016-0657-9.

[15] Diez-Fraile A, Lammens T, Tilleman K, Witkowski W, Verhasselt B, De Sutter P, Benoit Y, Espeel M, D'Herde K. Age-associated differential microRNA levels in human follicular fluid reveal pathways potentially determining fertility and success of in vitro fertilization. Hum Fertil 2014;17:90–8. https://doi.org/10.3109/14647273.2014.897006.

[16] Navakanitworakul R, Hung WT, Gunewardena S, Davis JS, Chotigeat W, Christenson LK. Characterization and small RNA content of extracellular vesicles in follicular fluid of developing bovine antral follicles. Sci Rep 2016;6:25486. https://doi.org/10.1038/srep25486.

[17] Hasan MM, Viil J, Lättekivi F, Ord J, Reshi QUA, Jääger K, Velthut-Meikas A, Andronowska A, Jaakma Ü, Salumets A, Fazeli A. Bovine follicular fluid and extracellular vesicles derived from follicular fluid alter the bovine oviductal epithelial cells transcriptome. Int J Mol Sci 2020;21:5365. https://doi.org/10.3390/ijms21155365.

[18] da Silveira JC, Winger QA, Bouma GJ, Carnevale EM. Effects of age on follicular fluid exosomal microRNAs and granulosa cell transforming growth factor-β signalling during follicle development in the mare. Reprod Fertil Dev 2015;27:897–905. https://doi.org/10.1071/RD14452.

[19] Gabryś J, Kij-Mitka B, Sawicki S, Kochan J, Nowak A, Łojko J, Karnas E, Bugno-Poniewierska M. Extracellular vesicles from follicular fluid may improve the nuclear maturation rate of in vitro matured mare oocytes. Theriogenology 2020;188:116–24. https://doi.org/10.1016/j.theriogenology.2022.05.022.

[20] Grzesiak M, Popiolek K, Knapczyk-Stwora K. Extracellular vesicles in follicular fluid of sexually mature gilts' ovarian antral follicles - identification and proteomic analysis. J Physiol Pharmacol 2020;71. https://doi.org/10.26402/jpp.2020.1.13. 10.26402/jpp.2020.1.13.

[21] Benedikter BJ, Bouwman FG, Vajen T, Heinzmann ACA, Grauls G, Mariman EC, Wouters EFM, Savelkoul PH, Lopez-Iglesias C, Koenen RR, Rohde GGU, Stassen FRM. Ultrafiltration combined with size exclusion chromatography efficiently isolates extracellular vesicles from cell culture media for compositional and functional studies. Sci Rep 2017;7:15297. https://doi.org/10.1038/s41598-017-15717-7.

[22] Akins EL, Morrisette MC. Gross ovarian changes during estrus cycle of swine. Am J Vet Res 1968;29:1953e7.

[23] Reshi QUA, Hasan MM, Dissanayake K, Fazeli A. Isolation of extracellular vesicles (EVs) using benchtop size exclusion chromatography (SEC) columns. Methods Mol Biol 2021;2273:201–6. https://doi.org/10.1007/978-1-0716-1246-0_14.

[24] Dissanayake K, Midekessa G, Lättekivi F, Fazeli A. Measurement of the size and concentration and zeta potential of extracellular vesicles using nanoparticle tracking analyzer. Methods Mol Biol 2021;2273:207–18. https://doi.org/10.1007/978-1-0716-1246-0_15.

[25] Midekessa G, Godakumara K, Ord J, Viil J, Lättekivi F, Dissanayake K, Kopanchuk S, Rinken A, Andronowska A, Bhattacharjee S, Rinken T, Fazeli A. Zeta potential of extracellular vesicles: toward understanding the attributes that determine colloidal stability. ACS Omega 2020;5:16701–10. https://doi.org/10.1021/acsomega.0c01582.

[26] Nečas D, Klapetek P. Gwyddion: an open-source software for SPM data analysis. Open Phys 2012;10:181–8. https://doi.org/10.2478/s11534-011-0096-2.

[27] Grzesiak M, Kaminska K, Bodzioch A, Drzewiecka EM, Franczak A, Knapczyk-Stwora K. Vitamin D3 metabolic enzymes in the porcine uterus: expression, localization and autoregulation by 1,25(OH)2D3 in vitro. Int J Mol Sci 2022;23:3972. https://doi.org/10.3390/ijms23073972.

[28] Théry C, Witwer KW, Aikawa E, et al. Minimal information for studies of extracellular vesicles 2018 (MISEV2018): a position statement of the International Society for Extracellular Vesicles and update of the MISEV2014 guidelines. J Extracell Vesicles 2018;7:1535750. https://doi.org/10.1080/20013078.2018.1535750.

[29] Raposo G, Stoorvogel W. Extracellular vesicles: exosomes, microvesicles, and friends. J Cell Biol 2013;200:373–83. https://doi.org/10.1083/jcb.201211138.

[30] Yuan C, Li Z, Zhao Y, Wang X, Chen L, Zhao Z, Cao M, Chen T, Iqbal T, Zhang B, Fan W, Wei Y, Li C, Zhou X. Follicular fluid exosomes: important modulator in proliferation and steroid synthesis of porcine granulosa cells. Faseb J 2021;35:e21610. https://doi.org/10.1096/fj.202100030RR.

[31] Cizmar P, Yuana Y. Detection and characterization of extracellular vesicles by transmission and cryo-transmission electron microscopy. Methods Mol Biol 2017;1660:221–32. https://doi.org/10.1007/978-1-4939-7253-1_18.

[32] Edwards RG. Follicular fluid. J Reprod Fertil 1974;37:189–219. https://doi.org/10.1530/jrf.0.0370189.

[33] Bairamukov V, Bukatin A, Landa S, Burdakov V, Shtam T, Chelnokova I, Fedorova N, Filatov M, Starodubtseva M. Biomechanical properties of blood plasma extracellular vesicles revealed by atomic force microscopy. Biology 2021;10:4. https://doi.org/10.3390/biology10010004.

[34] Sódar BW, Kittel Á, Pálóczi K, et al. Low-density lipoprotein mimics blood plasma-derived exosomes and microvesicles during isolation and detection. Sci Rep 2016;6:24316. https://doi.org/10.1038/srep24316.

[35] Brennan K, Martin K, FitzGerald SP, O'Sullivan J, Wu Y, Blanco A, Richardson C, Mc Gee MM. A comparison of methods for the isolation and separation of extracellular vesicles from protein and lipid particles in human serum. Sci Rep 2020;10:1039. https://doi.org/10.1038/s41598-020-57497-7.

[36] Gan C, Ao M, Liu Z, Chen Y. Imaging and force measurement of LDL and HDL by AFM in air and liquid. FEBS Open Bio 2015;5:276–82. https://doi.org/10.1016/j.fob.2015.03.014.

[37] Jamaludin NA, Thurston LM, Witek KJ, Meikle A, Basatvat S, Elliott S, Hunt S, Andronowska A, Fazeli A. Efficient isolation, biophysical characterisation and molecular composition of extracellular vesicles secreted by primary and immortalized cells of reproductive origin. Theriogenology 2019;135:121–37. https://doi.org/10.1016/j.theriogenology.2019.06.002.

[38] de Menezes-Neto A, Sáez MJ, Lozano-Ramos I, Segui-Barber J, Martin-Jaular L, Ullate JM, Fernandez-Becerra C, Borrás FE, Del Portillo HA. Size-exclusion

chromatography as a stand-alone methodology identifies novel markers in mass spectrometry analyses of plasma-derived vesicles from healthy individuals. J Extracell Vesicles 2015;4:27378. https://doi.org/10.3402/jev.v4.27378.

[39] Blanc L, Vidal M. New insights into the function of Rab GTPases in the context of exosomal secretion. Small GTPases 2018;9:95–106. https://doi.org/10.1080/21541248.2016.1264352.

[40] Machtinger R, Baccarelli AA, Wu H. Extracellular vesicles and female reproduction. J Assist Reprod Genet 2021;38:549–57. https://doi.org/10.1007/s10815-020-02048-2.

[41] Mobarak H, Heidarpour M, Lolicato F, Nouri M, Rahbarghazi R, Mahdipour M. Physiological impact of extracellular vesicles on female reproductive system; highlights to possible restorative effects on female age-related fertility. Biofactors 2019;45:293–303. https://doi.org/10.1002/biof.1497.